Liquid Crystals
Publication details, including instructions for authors and subscription information:
http://www.informaworld.com/smpp/title~content=t713926090

Unusual molecular packing within the low symmetry mesophases of alkyl- and alkoxy-acylhydrazinatonickel(II) liquid crystals

Martin Bellwood; Christina M. Buckley; Michael C. Holmes; RICHARD W. McCABE; Patrick D. Cookson

Online publication date: 06 August 2010

To cite this Article Bellwood, Martin , Buckley, Christina M. , Holmes, Michael C. , McCABE, RICHARD W. and Cookson, Patrick D.(1998) 'Unusual molecular packing within the low symmetry mesophases of alkyl- and alkoxy-acylhydrazinatonickel(II) liquid crystals', Liquid Crystals, 25: 1, 13 — 22
To link to this Article: DOI: 10.1080/026782998206452
URL: http://dx.doi.org/10.1080/026782998206452

LIQUID CRYSTALS, 1998, VOL. 25, NO. 1, 13–22

Unusual molecular packing within the low symmetry mesophases of alkyl- and alkoxy-acylhydrazinatonickel(II) liquid crystals

by MARTIN BELLWOOD*, CHRISTINA M. BUCKLEY†,
MICHAEL C. HOLMES, RICHARD W. M^{c}CABE†
and PATRICK D. COOKSON†

Department of Physics, Astronomy and Mathematics
†Department of Chemistry, University of Central Lancashire,
Preston PR1 2HE, UK

(*Received 3 October 1997; in final form 19 February 1998; accepted 25 February 1998*)

Three series of novel thermotropic metallomesogens have been synthesized and characterized using microscopy and DSC. Unexpected X-ray scattering is observed within all of the observed mesophases. Diffuse in-layer reflections are observed both at angles corresponding to approximately twice the molecular width and to the side-by-side separation of molecules within the nematic, SmA and SmC mesophases. Furthermore, the tilt angles within the SmC phases are observed to decrease as the terminal chain lengths decrease. Conoscopic observations show the SmC phases to be strongly biaxial as expected, but surprisingly, weak biaxiality is also observed within both the SmA and nematic mesophases. A model to explain the results is proposed, in which the cores remain orthogonal to the layers, whilst the overall molecular tilt necessary for SmC phase formation is provided by the contribution of the terminal alkyl chains to the overall molecular shape. IR spectroscopy is used to confirm the model.

1. Introduction

Metal-containing liquid crystals or metallomesogens have in recent years enjoyed an increase in interest from the scientific community and a number of reviews are available which demonstrate the variety and scope of the topic [1–5]. Metals show a variety of coordination geometries over and above the linear, trigonal and tetrahedral geometries of carbon and therefore metallomesogenic systems provide less frequently encountered ordered environments in which to study both the metal and complexing organic ligand. The high electron density of the metal centre may strongly modify properties such as the polarizability, birefringence and dielectric constant of the materials. Transition metal complexes are often vividly coloured, and this property may also be exploited to provide ordered coloured dopants for device application; ultimately, pure metallomesogenic display materials which do not rely on dopants or filters should become available.

The twin problems often encountered with metallomesogens are their high transition temperatures and the tendency towards decomposition compared with organic liquid crystals, but steps can be taken to reduce these effects. For example, increasing the structural anisotropy, using mixtures and altering the metal centre are common strategies.

An interesting property of metallomesogens is that where the metal is incorporated into a ring within the central core the molecules are usually wider than those of their organic counterparts. Thus there is a stronger inherent biaxiality on a molecular level and a greater potential for bias to rotation about the molecular long axis. There are two reasons why metallomesogenic molecules would exhibit biaxiality: (i) steric hindrance, since the molecules are sufficiently anisotropic that their shape causes hindrance to rotation about the molecular axes [6–11], and (ii) intermolecular interactions between adjacent molecules within the mesophase.

Studies of columnar [12–16] and other low symmetry (N, SmA and SmC phases) [17–25] metallomesogenic systems using experimental techniques as diverse as NMR, X-ray diffraction, EXAFS, EPR, diamagnetic susceptibility measurements and conoscopy have revealed evidence of intermolecular metal–ligand or metal–metal interactions. Such interactions seem to appear principally within systems which have a square planar (copper, nickel, palladium or platinum) or a square pyramidal (vanadyl V=O moiety) metal centre complexed to bidentate ligands with donor NN, NO, OO, OS or SS heteroatoms; the salicylaldimate-type systems in particular provide well studied examples [1–5].

*Author for correspondence.

The metallomesogens reported here are nickel(II) complexes of the *N*-methylidene-4-*n*-alkoxybenzoylhydrazinato ligand **1**, the *N*-methylidene-4-*n*-alkylbenzoylhydrazinato ligand **2**, and the *N*-methylidene-4-*n*-alkoxy-3-fluorobenzoylhydrazinato ligand **3**.

For the alkoxy series **1**, homologues with 4–12, 14, 20 and 22 carbon atoms in the terminal chains were synthesized by synthetic routes which have been previously reported [26–29]. These complexes display nematic phases at short terminal chain lengths ($n \leqslant 7$), nematic and SmC phases at medium chain lengths ($n = 8, 9, 10$) and SmC phases at long chain lengths ($n \geqslant 11$). A clear 'odd-even' effect is observed in the clearing temperatures of these alkoxy complexes. Interestingly, the complex **1**: $R = C_{10}$ displayed the unusual property of multiple melting; that is, on first heating, the 'virgin' sample melted to the SmC phase at 135°C, whilst on subsequent heating cycles melting occurred at 141°C. This implies a less stable crystal structure when the sample is recrystallized from solvent than when it is cooled from the liquid phase. Whilst rare, this phenomenon is not unique amongst metallomesogens [30, 31].

For the alkyl series **2**, homologues with 6, 8, 10 and 12 carbon atoms in the terminal chains were synthesized [29] and these displayed SmA phases only. The shortest chain analogue ($n = 6$) displayed a monotropic SmA phase.

For the *meta*-fluorinated alkoxy series **3**, homologues with 6, 8, 12 and 14 carbon atoms in the terminal chains were synthesized [29]. These complexes displayed SmA phases at short terminal chain lengths ($n = 6, 8$) or SmC phases at long terminal chain lengths ($n = 12, 14$).

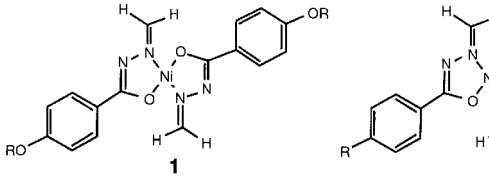

1

2

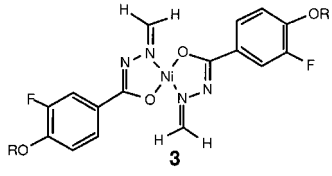

3

$R = C_nH_{2n+1}$

The mesophases and transition temperatures of the above complexes are listed in table 1. These systems displayed typical optical textures associated with their mesophases when initially studied by polarized light microscopy. The nematic phases of the complexes **1** displayed classic nematic schlieren textures and when stressed displayed the marbled nematic texture. The SmA phases of the complexes **2** and **3** were characterized by focal conic fan textures which grew out of bâtonnets

Table 1. Transition temperatures (°C) and mesophases of the complexes discussed. Temperatures were measured by microscopy and confirmed by DSC.

Complex	Phase transitions
Alkoxy	
1: $R = C_4$	Cr $\overset{203}{\underset{187}{\rightleftharpoons}}$ N $\overset{207}{\longrightarrow}$ I
1: $R = C_5$	Cr $\overset{159\text{–}61}{\underset{144}{\rightleftharpoons}}$ N $\overset{187}{\longrightarrow}$ I
1: $R = C_6$	Cr $\overset{161}{\underset{155}{\rightleftharpoons}}$ N $\overset{187}{\longrightarrow}$ I
1: $R = C_7$	Cr $\overset{139}{\underset{122}{\rightleftharpoons}}$ N $\overset{170}{\longrightarrow}$ I
1: $R = C_8$	Cr $\overset{159}{\underset{153}{\rightleftharpoons}}$ SmC $\overset{168}{\longrightarrow}$ N $\overset{174}{\longrightarrow}$ I
1: $R = C_9$	Cr $\overset{142}{\underset{122}{\rightleftharpoons}}$ SmC $\overset{163}{\longrightarrow}$ N $\overset{167}{\longrightarrow}$ I
[a] **1**: $R = C_{10}$	Cr $\overset{141}{\underset{122}{\rightleftharpoons}}$ SmC $\overset{167}{\longrightarrow}$ N $\overset{183}{\longrightarrow}$ I
1: $R = C_{11}$	Cr $\overset{127}{\underset{122}{\rightleftharpoons}}$ SmC $\overset{157}{\longrightarrow}$ I
1: $R = C_{12}$	Cr $\overset{125}{\underset{112}{\rightleftharpoons}}$ SmC $\overset{164\text{–}5}{\longrightarrow}$ I
1: $R = C_{14}$	Cr $\overset{133}{\underset{118}{\rightleftharpoons}}$ SmC $\overset{155}{\longrightarrow}$ I
1: $R = C_{20}$	Cr $\overset{131}{\underset{117}{\rightleftharpoons}}$ SmC $\overset{141}{\longrightarrow}$ I
1: $R = C_{22}$	Cr $\overset{124}{\underset{118}{\rightleftharpoons}}$ SmC $\overset{129}{\longrightarrow}$ I
Alkyl	
[b] **2**: $R = C_6$	Cr $\overset{146}{\longrightarrow}$ I; I $\overset{132}{\longrightarrow}$ SmA $\overset{112}{\longrightarrow}$ Cr
2: $R = C_8$	Cr $\overset{128}{\underset{125}{\rightleftharpoons}}$ SmA $\overset{137}{\longrightarrow}$ I
2: $R = C_{10}$	Cr $\overset{117}{\underset{108}{\rightleftharpoons}}$ SmA $\overset{138}{\longrightarrow}$ I
2: $R = C_{12}$	Cr $\overset{122}{\underset{117}{\rightleftharpoons}}$ SmA $\overset{128}{\longrightarrow}$ I
mF-Alkoxy	
3: $R = C_6$	Cr $\overset{169}{\underset{165}{\rightleftharpoons}}$ SmA $\overset{176}{\longrightarrow}$ I
3: $R = C_8$	Cr $\overset{153\text{–}4}{\underset{148\text{–}7}{\rightleftharpoons}}$ SmA $\overset{170}{\longrightarrow}$ I
3: $R = C_{12}$	Cr $\overset{143}{\underset{138}{\rightleftharpoons}}$ SmC $\overset{157}{\longrightarrow}$ I
3: $R = C_{14}$	Cr $\overset{139}{\underset{135}{\rightleftharpoons}}$ SmC $\overset{149}{\longrightarrow}$ I

[a] Complex exhibits 'multiple melting'—see text for explanation.
[b] Monotropic SmA phase.

on cooling from the isotropic phase. The SmC phases of complexes **1** and **3** were characterized by the appearance of SmC schlieren and sanded schlieren textures. DSC was used to measure the mesophase transition temperatures and enthalpies.

2. X-ray scattering

The X-ray patterns of these complexes may be split into two parts—the low Q and the high Q regions. Layer features, i.e. those which correspond to the layer separation, are from here on referred to as being in the low Q region of the diffraction patterns. In-layer features, i.e. those which correspond to molecular separation within the layers, are referred to as in the high Q region.

2.1. *High Q X-ray scattering: in-layer features*

In all of the mesophases displayed by complexes **1**, **2** and **3**, two diffuse features are observed in the high Q region of the diffraction patterns; the scattering features and calculated molecular lengths assuming an all-*trans*-chain configuration are given in tables 2, 3 and 4, respectively. The short chain homologues of the alkoxy series **2** tended to decompose before reliable scattering in the high Q region could be obtained.

Table 2. X-ray scattering data and calculated molecular lengths L for the alkoxy complexes **1**.

	Scattering features/Å			
Complex	Molecular length L	Low Q region (d_o)	High Q region (in-layer features)	
1: $R = C_4$ (N)	26·6	[a]—	[a]—	[a]—
1: $R = C_5$ (N)	29·5	28 ± 1	[a]—	[a]—
1: $R = C_6$ (N)	31·7	29·1 ± 0·5	15·6 ± 0·5	[a]—
1: $R = C_7$ (N)	34·3	32 ± 1	15·7 ± 0·5	5·1 ± 0·5
1: $R = C_8$ (N)	36·6	34 ± 1	16·2 ± 0·5	5·0 ± 0·5
1: $R = C_8$ (SmC)	36·6	[b]	16·0 ± 0·5	4·5 ± 0·5
1: $R = C_9$ (N)	39·2	36·7 ± 0·5	15·2 ± 0·5	5·2 ± 0·5
1: $R = C_9$ (SmC)	39·2	[b]	14·9 ± 0·5	5·2 ± 0·5
1: $R = C_{10}$ (SmC)	41·6	39 ± 1	—	—
1: $R = C_{10}$ (SmC)	41·6	[b]	15·6 ± 0·5	4·5 ± 0·5
1: $R = C_{11}$ (SmC)	44·2	[b]	14·9 ± 0·5	4·8 ± 1·0
1: $R = C_{12}$ (SmC)	46·6	[b]	16·4 ± 0·5	5·2 ± 0·5
1: $R = C_{14}$ (SmC)	50·2	[b]	16·3 ± 0·5	4·5 ± 0·5
1: $R = C_{20}$ (SmC)	64·9	[b]	15·8 ± 0·5	5·0 ± 0·5
1: $R = C_{22}$ (SmC)	69·9	[b]	16·2 ± 0·5	5·2 ± 0·5

[a] Sample decomposes before reliable scattering can be taken.
[b] See table 5.

Table 3. X-ray scattering data and calculated molecular lengths L for the SmA phases of the alkyl complexes **2**.

	Scattering features/Å			
Complex	Molecular length L	Low Q region (d_o)	High Q region (in-layer features)	
2: $R = C_6$ (SmA)	29·7	29 ± 1	15·5 ± 0·5	5·0 ± 0·5
2: $R = C_8$ (SmA)	34·5	33 ± 1	15·5 ± 0·5	5·5 ± 0·5
2: $R = C_{10}$ (SmA)	39·5	37 ± 1	15·5 ± 0·5	—
2: $R = C_{12}$ (SmA)	44·4	43 ± 1	16·0 ± 0·5	5·0 ± 0·5

Table 4. X-ray scattering data and calculated molecular lengths L for the *m*F-alkoxy complexes **3**.

	Scattering features/Å			
Complex	Molecular length L	Low Q region (d_o)	High Q region (in-layer features)	
3: $R = C_6$ (SmA)	31·7	30 ± 1	14·9 ± 0·5	5·1 ± 0·5
3: $R = C_8$ (SmA)	36·6	34 ± 1	16·0 ± 1	5·4 ± 0·5
3: $R = C_{10}$ (SmC)	46·6	[a]	14·8 ± 0·5	5·2 ± 0·5
3: $R = C_{12}$ (SmC)	50·2	[a]	15·3 ± 0·5	5·0 ± 0·5

[a] See table 5.

Figure 1 clearly shows both these diffuse scattering features, as exhibited by the SmA phases of the alkyl complexes **2**: $R = C_6$ and **2**: $R = C_{12}$. The 1D profiles are taken directly from the 2D patterns shown along the superimposed black lines. The features in the region (a) are from the low Q layer spacings and in these cases were deliberately overexposed in order that the high Q, in-layer features (b) and (c) were more readily observed.

The first and most prominent diffuse feature (b) occurs at *c.* 16 Å, approximately twice that expected from a calamitic molecule of width 8 Å. The second, less prominent diffuse feature (c) occurs at *c.* 5 Å. This feature could be due to two possible causes: liquid-like alkyl chain scattering or an average side-by-side molecular separation. If the scattering is a result of side-by-side separation then a degree of biaxiality within the SmA phase is implied.

2.2. *Low Q X-ray scattering: layer features*

The second scattering features of interest are those in the low Q region displayed by the SmC mesophases of the alkoxy complexes **1** and the *m*F-alkoxy complexes **3**, shown in table 5. For each individual complex, the measured layer spacing and tilt angle remain essentially constant within experimental error on cooling, as expected from a SmC phase preceding an isotropic or nematic phase.

The layer tilt angles θ were calculated from the experimentally observed layer spacings d_o and the molecular lengths L presented in tables 2 and 4, where

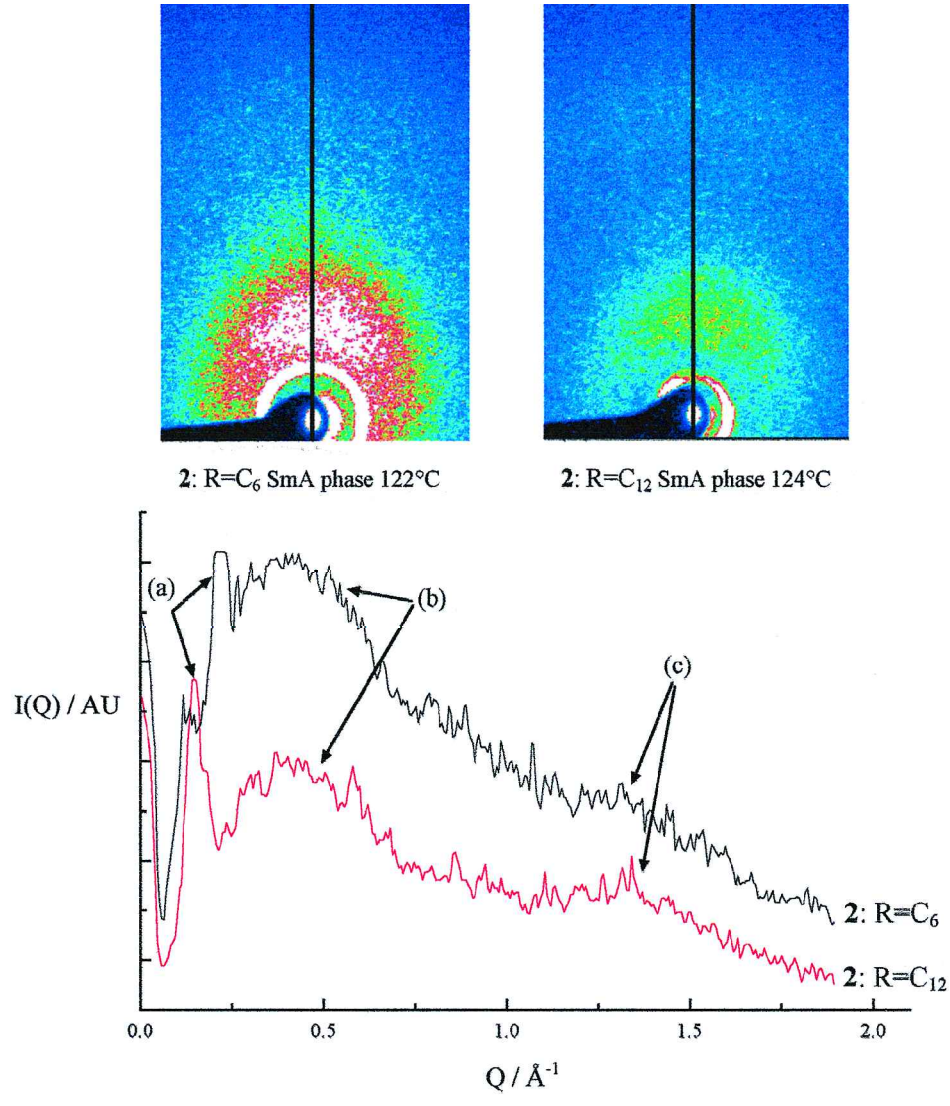

Figure 1. X-ray scattering taken on cooling from the SmA phases of the (monotropic) C_6 and C_{12} alkyl complexes **2**. The 1D patterns are taken directly from the 2D patterns shown along the superimposed black lines. The low Q layer scattering (a) and high Q diffuse in-layer scattering features (b) and (c) are shown on the 1D plot.

Table 5. Measured layer spacings and calculated tilt angles (in parentheses) as a function of reduced temperature for the alkoxy and *m*F-alkoxy complexes which exhibit SmC phases.

Reduced temperature /°C	Complex and smectic layer spacing/Å (tilt angle θ/°)								
	1: $R=C_{22}$	**1**: $R=C_{20}$	**1**: $R=C_{14}$	**1**: $R=C_{12}$	**1**: $R=C_{11}$	**1**: $R=C_{10}$	**1**: $R=C_{8}$	**3**: $R=C_{14}$	**3**: $R=C_{12}$
T^*	49·1 ± 0·5 (45·4)	48·6 ± 0·5 (41·5)	42·2 ± 0·5 (32·8)	40·5 ± 0·5 (29·6)	36·7 ± 0·5 (33·9)	37·9 ± 0·5 (24·3)	32·7 ± 0·5 (26·7)	41·5 ± 0·5 (34·2)	40·7 ± 0·5 (29·1)
T^*-5	49·4 ± 0·5 (45·0)	48·2 ± 0·5 (42·0)	42·1 ± 0·5 (33·0)	39·5 ± 0·5 (32·0)	37·6 ± 0·5 (31·7)	38·3 ± 0·5 (23·0)	33·1 ± 0·5 (25·3)	42·0 ± 0·5 (33·2)	41·0 ± 0·5 (28·4)
T^*-10	51·4 ± 0·5 (42·7)	49·1 ± 0·5 (40·8)	42·1 ± 0·5 (33·0)	39·5 ± 0·5 (32·0)	38·5 ± 0·5 (29·4)	38·6 ± 0·5 (21·9)	33·6 ± 0·5 (23·4)	42·4 ± 0·5 (32·4)	41·2 ± 0·5 (27·6)

$\theta = \cos^{-1}(d_o/L)$. L was calculated assuming an all-*trans*-configuration of the terminal alkyl chains. The values of θ are given at consistent reduced temperatures for meaningful comparisons between members of the series, where T^* is the temperature of the SmC → I or the SmC → N transition. When the homologous series as a whole is considered, it can be seen from table 5 that the tilt angle decreases as the terminal chain length decreases. Considering the alkoxy series **2**, which has the largest range of SmC members, this trend can be seen quite clearly. The layer spacings and hence tilt angles of the *m*F-alkoxy complexes **3**: $R=C_{12}$ and **3**: $R=C_{14}$ are comparable to those of their alkoxy analogues.

The layer scattering from the SmA phases of complexes **2** and **3** was as expected. Intense rings (or Bragg peaks in aligned samples) occur in a 1 : 2 ratio, corresponding to a monolayer arrangement of molecules.

Scattering from the nematic phases of complexes **1** displayed very sharp arcs at low Q values corresponding to the molecular lengths. This observation indicated a considerable degree of cybotacticity, i.e. localized layering within the nematic phase. Interestingly, for the complexes **1**: $R=C_8, C_9, C_{10}$ these arcs were never observed to split into four spots as is common in cybotactic nematics preceding a SmC phase.

3. Conoscopic observations

The optical interference figures proved difficult to obtain for a variety of reasons. The stage was open to the air so that the samples were subject to temperature fluctuations at elevated temperatures. Uniformity of the sample thickness relied on coverslip quality, and whilst better results were obtained with thicker samples these proved more difficult to align. Field alignment of the samples proved difficult due to the experimental arrangement of the conoscope, and where applied proved too weak to affect the samples. This lack of any external aligning force meant that any biaxiality demonstrated by the samples was not field induced, but arose from an intrinsic system biaxiality.

As expected, the alkoxy and *m*F-alkoxy complexes that displayed SmC phases were strongly biaxial and exhibited conoscopic figures with their isogyres clearly separated.

The observation of slightly separated isogyres when studying the SmA phase complexes was surprising. Thin samples of the alkyl complexes displayed clearly separated isogyres compared with MBBA, a uniaxial reference sample, although the isogyres were not as fully separated as for the biaxial SmC phase complexes. This separation would seem to indicate a degree of biaxiality within the SmA phases of these mesogens.

Biaxial smectic A (SmA_b) phases are uncommon. Examples have typically wide molecules and exhibit a bias to rotation about their long axes resulting in a preferred in-plane orientation of the shorter axes, thus losing the isotropic distribution of the molecules within the layers. The phase has a local D_{2h} symmetry, is orthorhombic and therefore optically biaxial. The systems studied here are clearly calamitic in nature and are far less biaxial on a molecular level than any of the theoretically predicted or experimentally observed SmA_b systems; it is therefore surprising to see them exhibit any degree of biaxiality. The origin of the biaxiality is thought unlikely to be of a purely steric nature and other causes of this effect must be sought.

Similar observations of slightly separated isogyres within the nematic phases of the alkoxy complexes **1** are also noted, although for the shorter terminal chain complexes (**1**: $R=C_{n<7}$) the measurements could not be made, as decomposition occurred rapidly before a suitable region was obtained for study. Again, this separation indicated biaxiality within the supposedly uniaxial nematic phase. Biaxial nematic phases have been observed experimentally, but tend to occur in sanidic systems in which the length/width ratio of the central molecular core is considerably greater than in the systems studied here [32].

Chandrasekhar noted [32] that when viewing the optical textures of biaxial nematics, disclinations of

strength ± 1 in the schlieren textures were uncommon and textures often consist only of disclinations of strength $\pm 1/2$. There is a noticeable predominance of $\pm 1/2$ disclinations observed in the optical textures of the nematic phases of complexes **1**; however both types of disclinations are observed and this again may be taken to indicate only weak biaxiality within the nematic phase.

4. Discussion

The experimental observations must now be explained: the outer ~ 5 Å and inner ~ 16 Å diffuse X-ray scattering features, the decreasing tilt angle with decreasing chain length in the SmC phases, and the results from the conoscopic observations.

The separation of the isogyres seen in the conoscopy experiments indicates the presence of two optical axes and therefore a degree of biaxiality within the SmA phases; this, together with the ~ 5 Å scattering feature (an indication of a side-by-side association between molecules), implies biased rotation about the molecular long axes and therefore a degree of biaxiality within the N and SmA phases. The ~ 16 Å scattering feature and the decrease in tilt angle taken together indicate an unusual packing of molecules within the mesophases. The calamitic nature of the molecules makes it reasonable to assume that the origin of these effects is not entirely steric.

4.1. *The nature of the intermolecular interactions*

It has already been mentioned that intermolecular interactions are not uncommon in the liquid crystalline phases of metallomesogenic systems. It is proposed that a metal–ligand association between adjacent molecules occurs in the acylhydrazinatonickel(II) complexes studied here. The observation of anomalous magnetic behaviour in dilute solutions of the non-mesogenic *bis*(*N*-methylsalicylaldimine)nickel(II) complexes [33] was explained in terms of a polymeric association between neighbouring molecules involving a Ni–O···Ni–O association in which the nickel has a distorted octahedral structure involving $4s4p^3 3d^2$ bonding. Within a mesophase such an association between molecular cores would be more likely to occur. This would increase the rotational bias about the molecular long axis, thus satisfying the conoscopic observations by providing a degree of biaxiality to the system. A side-by-side arrangement would also reinforce the diffuse 5 Å X-ray scattering.

An important consideration resulting from such a model is that the close proximity of adjacent molecules would both affect the flexibility of the terminal chains and limit chain and molecular rotations, thus allowing local steric effects, which would otherwise be 'smeared out', to become important.

4.2. *Packing within the mesophases*

As the nematic phase showed a tendency towards cybotacticity and therefore to form pseudo-layers within the mesophase, for the purpose of the following model it may essentially be thought of as being similar to the SmA phase.

In order to satisfy the diffuse 16 Å scattering, the molecules within the N or SmA mesophases must differ from their nearest in-layer neighbours. It is proposed that Ni–O···Ni–O interactions cause enough rotational bias to allow steric effects imposed by the core *N*-methylidene ($>N{=}CH_2$) groups to hinder molecular movements, giving rise to an alternate staggering of the molecules within the layers. The models given in figure 2 show the relationship between the main core and these side groups, and the effect on the in-layer packing. Figures 2(*a*) and 2(*b*) show possible arrangements of short chain complexes that satisfy the observed scattering. Figure 2(*a*) shows all the molecules in the same orientation; figure 2(*b*) shows molecules randomly oriented about the molecular long axis. At the short chain lengths shown (N and SmA phases), the orientation of the molecules is likely to be irrelevant. Whatever the molecular arrangement the staggering effect is still observed leaving adjacent molecules different. As the chain length increases and the SmC phase is stabilized, the orientation of the molecules becomes progressively more important.

If the molecules are arranged as shown in figure 2(*b*), it is very easy to see that at some critical chain length the chains would become arranged crosswise, and a random molecular orientation within the layer would become sterically unfavourable. Thus at longer chain lengths and within the SmC phase, the molecules are *less* likely to be randomly oriented and would adopt the orientation shown in figure 2(*a*).

Two points must be stressed: (i) the in-plane diffuse 5 Å scattering cannot be unambiguously assigned as due to a side by side arrangement of the molecules, and (ii) the molecules must still rotate about their long axes, otherwise a phase of higher order, e.g. the E phase, would be observed. The in-plane distribution is liquid-like, and the individual molecules do not have defined positional order or orientations. Rotation about the long axes is just heavily biased by a combination of the attractive intermolecular interactions described and chain interactions at longer chain lengths.

The model may now be directly extended to the SmC phase, where it is proposed that the cores retain their orthogonality. If the cores are allowed to tilt within the SmC phase then two possible arrangements, shown schematically in figures 2(*c*) and 2(*d*) may occur. Whilst the arrangement in figure 2(*c*) would pack favourably within layers there is no difference between adjacent

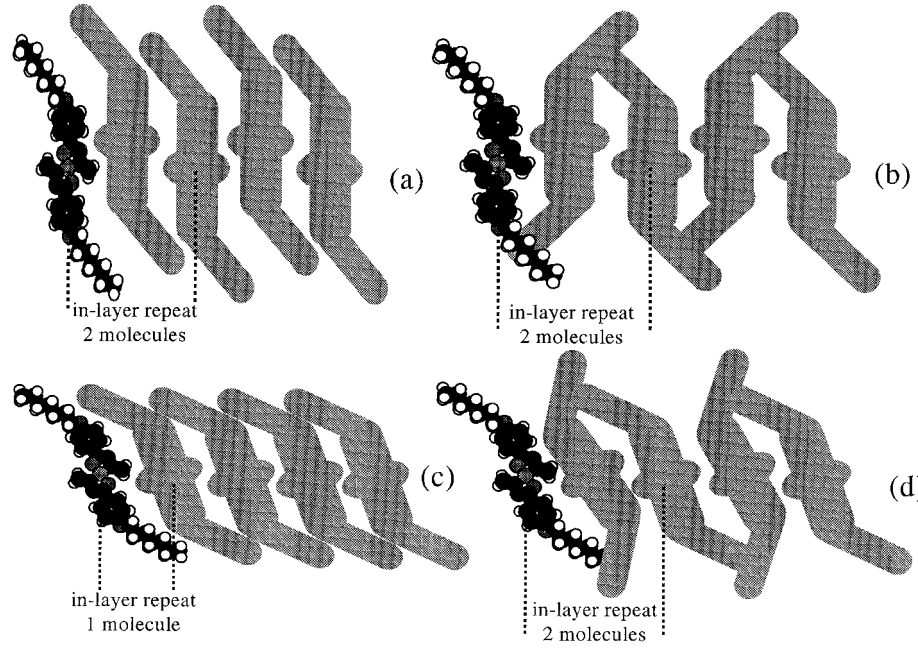

Figure 2. Possible arrangements for the in-layer packing, in which the cores are either tilted or normal to the layers. A full explanation is given in the text for each of the arrangements.

molecules and thus the diffuse 16 Å scattering would not be observed. The arrangement shown in figure 2(*d*) would satisfy the observed 16 Å scattering, but would result in unfavourable packing of the terminal chains within the layers at the chain lengths necessary for SmC formation. Assuming the cores are orthogonal to the layers in the SmC phase, figure 3 shows schematically how for long, medium and short terminal alkyl chains the respective tilt angles θ_l, θ_m and θ_s decrease in a manner consistent with that observed experimentally for the systems under consideration.

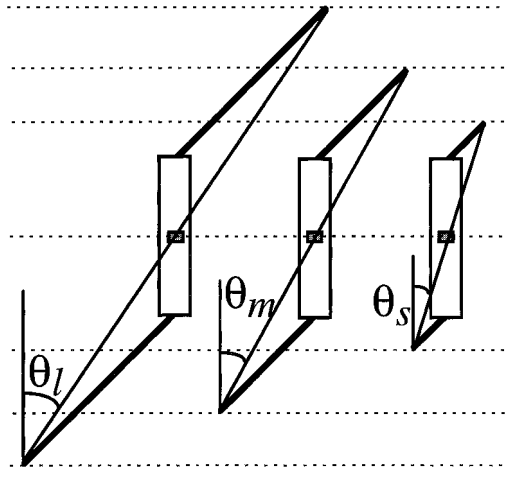

Figure 3. Schematic representation of the tilt angles at long, medium and short chain lengths (θ_l, θ_m and θ_s respectively) within the SmC phase. The retention of core orthogonality within the mesophase allows the chain length to dominate the observed tilt angles.

Predicted layer spacings from simple space filling models in the arrangement shown in figure 2(*a*) are in very close agreement with those observed and presented in table 5. The predictions are less accurate for the longest chain complexes **1**: $R = C_{20}$ and **1**: $R = C_{22}$, but the space filling models assume an all-*trans*-conformation for the terminal chains and only a small amount of chain deformation is needed to obtain spacings, and thus tilt angles, closer to those observed.

Some models of the SmC phase dealing with calamitic molecules have regarded the outboard dipoles provided by the terminal chain oxygens as necessary for mesophase formation, although the limitations of such models have been dealt with elsewhere [34]. If such outboard dipoles caused the cores to tilt, then an arrangement as shown in figure 2(*c*) would occur, with all the dipoles arranged in the same direction, and would not fully account for the diffuse high Q scattering. Finally, if the cores are allowed to tilt then the layer spacings would be considerably smaller than those actually observed. Whilst dipolar effects are not totally discounted when considering mesophase formation, they are not considered important within the confines of the model presented here.

4.3. *Infrared spectroscopic studies*

Infrared spectroscopy (IR) studies were carried out to provide extra information regarding the molecular structure within the mesophase. Whereas microscopy, conoscopy and scattering techniques give information about the bulk phase, IR gives information specific to the molecules within the phase. If there is any donative

effect between adjacent molecular orbitals as described, then there should be a change in the strength of the bond detectable by IR.

El Sayed and Iskander [35] first reported the complexation of differently substituted aroyl hydrazones (R–CH=N–NHCO-R') with nickel(II) and copper(II) salts to give (non-mesogenic) complexes with a core structure similar to the mesogens under study in this report. They assigned an IR band at 1602 cm^{-1} to the stretching vibration mode within the ligand C=N=N=C unit. This vibrational mode occurs at 1602 cm^{-1} in the alkoxy **1**, 1606 cm^{-1} in the alkyl **2** and 1609–10 cm^{-1} in the *m*F-alkoxy **3** complexes. Any interactions between an oxygen within this molecule and a nickel in an adjacent one should be accompanied by a change to this absorption band on cooling from the isotropic liquid through the mesophase into the solid phase, as the interactions become stronger.

Further information regarding the role of the terminal chains during mesophase formation should also be observed. It is well known from hydrocarbons that in the solid phase the all-*trans*-conformation of the chain is energetically most favourable. In the liquid phase the chain gradually folds and distorts with increasing temperature, but near the solid–liquid transition the all-*trans*-conformation is still retained [36]. IR studies of liquid crystals have revealed changes in the terminal chain rocking and skeletal vibrations at the Cr → LC transition; and less frequently changes at the LC → I transition [37–39]. (It must be remembered that the Cr → LC transition is strongly first order compared with LC → I and thus the majority of changes in motional freedom and intermolecular interactions occur here.)

The sodium chloride cell plates were cleaned and polished before use—polishing also aids liquid crystal alignment. The samples were spread evenly across the cell and heated to the isotropic phase prior to measurements to allow an even spread of liquid crystal across the cell. The cell was held during this initial heating in such a manner that the liquid flowed under gravity in the direction of polishing, which further flow-aligned the sample. The sample in the cell was then reheated to the isotropic phase and allowed to cool, and spectra were taken at 2–3°C intervals over the region of interest.

The spectra shown in figure 4 were obtained from the complex **3**: $R = C_6$ on cooling from the isotropic phase through the SmA and into the solid phase. The solid state spectrum obtained from the recrystallized sample prepared in a KBr disk is also shown for comparison.

The ligand stretching vibration mode assigned by El Sayed and Iskander [35] is shown, along with other absorption bands of interest. As can be seen, over the LC/I transition there is a small increase of *c.* 1–2 cm^{-1} in the ligand C=N=N=C vibration and a larger increase over the LC/Cr phase transition of *c.* 4–5 cm^{-1} occurs. The band also becomes progressively sharper on cooling from the disordered to the ordered phases, implying an increase in the order of the group or bonds within the group. This is consistent with an associative model involving the group.

Interestingly, the alkyl complexes **2** display characteristic sharpening, but a considerably smaller shift in

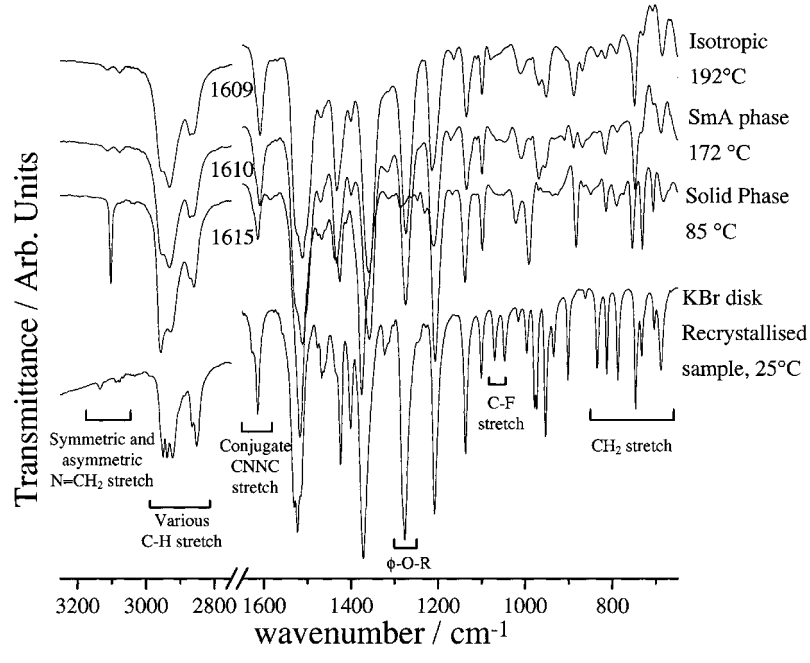

Figure 4. Infrared spectra obtained from the *m*F-alkoxy complex **3**: $R = C_6$ on cooling from the isotropic phase through the mesophase into the solid phase, and from the recrystallized sample in KBr disk form. The sample and cell were prepared in the manner described in the text. Some regions of interest are marked on the spectra.

the band on cooling through the I → SmA → Cr phase sequence than the alkoxy and *m*F-alkoxy series. The implication is a stronger association between molecules and a correspondingly smaller change in molecular organization at the phase transitions in the alkyl mesophases than for either the alkoxy or *m*F-alkoxy complexes. This is probably due to a combination of lower mesophase temperatures and smaller disruptive effects from the terminal chains.

The $>CH_2$ rocking bands at $\sim 720\,cm^{-1}$ smear out in the LC phases, but do not completely disappear in the I phase. The weak $>CH_2$ bending bands in the region ~ 1300–$1200\,cm^{-1}$ should merge into two broad bands in the LC and I phases [38], indicative of many rotational isomers existing in the liquid phases, whereas principally stable *trans*-conformers exist in the solid chains. Much of this 'fine structure' is retained in the liquid phases as distinct weak bands or shoulders on broader bands. Similarly other $>CH_2$ rocking and twisting bands in the region ~ 1400–$1100\,cm^{-1}$ do not broaden or disappear completely as may be expected in the liquid phases, implying that a greater degree of order is retained within the chains than is observed in other LC systems. This is consistent with a model in which the molecules are not allowed free rotation about their long axes and in which the terminal chains play an important role.

A sharp band at $1096\,cm^{-1}$ in the *m*F-alkoxy complexes, assigned as the C–F stretching band, altered neither position nor intensity significantly in either the Cr, LC or I phases, indicating that the fluorine plays no part in any association.

The *N*-methylidene (N=CH_2) C–H symmetric and asymmetric stretching bands are assigned at 3110–$3100\,cm^{-1}$ depending on the system studied. In the spectra shown, this band, along with the terminal ϕ-O–R oxygen stretch band at $1280\,cm^{-1}$, illustrates an interesting effect. On cooling into the solid phase, crystal growth is seeded on the cell windows in such a way that the orientation of the molecules effectively shields certain bonds from the incident radiation. Molecules in the KBr disk however are randomly orientated and allow all absorptions, and so differently prepared samples give different spectra. Hence in the sample cooled to the Cr phase, both the asymmetric C–H stretch and the ϕ-O–R oxygen stretch disappear, whereas in the KBr disk sample both are clearly visible.

Whilst these IR spectra do not provide unambiguous evidence that an intermolecular association such as that proposed occurs, they do provide good supporting evidence.

5. Experimental details

Conoscopic measurements were carried out using a Vickers M72 biological compound polarizing microscope with an in-built Bertrand lens. To ensure the sample was located at the condenser focal point and the objective was as close to the sample as possible, a specially built thin Linkam hot stage and TMS92 programmable temperature controller was used. Although the sample was open to the air and temperature accuracy was considerably reduced, by returning the conoscope to its more usual microscope function it was easy to ensure that samples were in the appropriate mesophase before conoscopic observations were carried out.

X-ray diffraction measurements were carried out using a Hiltonbrooks DG1 or a Phillips PW1830 X-ray generator. A Phillips fine focus X-ray tube (Cu K_α) with nickel filter at 45 kV and 25 mA and a pinhole camera point collimated to 0·3 mm were used in both cases. Samples were heated using a Linkam X-ray hot stage and PR600 temperature controller. The temperature accuracy was considered no worse than ±1°C at 140°C. Detection was by a Photonic Science Xr50 detector connected to a DIS3000 imaging control system, or by stacked X-ray film. Additionally, the synchrotron X-ray source at Daresbury was used to establish layer d_o spacings. Data were collected at Station 7.2 using a film detection system, and Station 8.2 using an electronic area detector. The temperature in this case was regulated by a Linkam TMS91 controller attached to a THM600 sample stage; again, temperature accuracy was considered no worse than ±1°C.

FTIR spectra were recorded on Mattson Instruments Galaxy or Polaris Icon spectrometers. The samples were held in an electrically heated cell, whose temperature was controlled by an in-house constructed power unit and whose accuracy was no worse than ±2°C at the clearing temperatures. The cells were made of single crystal sodium chloride plate windows and completed with 10 μm plastic spacers.

6. Conclusions

The homologous liquid crystalline series presented show clear evidence of unusual in-layer packing within all of their low symmetry mesophases. This occurs as a result of intermolecular interactions which slow rotation about the molecular long axes sufficiently to allow steric effects to dominate. The most unusual aspect of these systems is the observation of weak biaxiality within the SmA phases of the alkyl and *m*F-alkoxy complexes. Previous reports of biaxiality in SmA phases lead one to suppose that such an effect is almost exclusively steric, caused by a strong biaxiality on the molecular level in systems more appropriately described as sanidic, whereas the systems studied here are quite clearly calamitic in nature. Biaxiality within the nematic phase is also observed, again unexpected with calamitic molecules. In order to confirm unambiguously the proposed model,

further work must be undertaken. Far IR studies of the Ni–O or Ni–N bonds could be carried out, and EXAFS studies may also be utilized to confirm the metal environment.

Such intermolecular metal–ligand interactions may be more common than expected and, if exploited, could lead to the enhancement of inherent biaxiality within metallomesogenic systems and the development of novel materials.

We would like to thank the CLRC for beam-time at the SRS, Daresbury, in order to make the SAXS measurements. M.B. and C.M.B. are grateful to the University of Central Lancashire for providing studentships. M.B. would like to dedicate this work to the memory of Tony Rybaczek, a good friend.

References

[1] Giroud-Godquin, A. M., and Maitlis, P. M., 1991, *Angew. Chem.*, **30,** 375.
[2] Espinet, P., Esteruelas, M. A., Oro, L. A., Serrano, J. L., and Sola, E., 1992, *Coord. Chem. Rev.*, **117,** 215.
[3] Bruce, D. W., 1992, *Inorganic Materials*, edited by D. W. Bruce and D. O'Hare (Wiley), Chap. 8.
[4] Hudson, S. A., and Maitlis, P. M., 1993, *Chem. Rev.*, **93,** 861.
[5] Serrano, J. L., 1996, *Metallomesogens—Synthesis, Properties, and Applications*, edited by J. L. Serrano (VCH Verlag).
[6] Chandrasekhar, S., Sadashiva, B. K., Ratna, B. R., and Raja, V. N., 1988, *Pramana J. Phys.*, **30,** L491.
[7] Espinet, P., Perez, J., Marcos, M., Ros, M. B., Serrano, J. L., Barbera, J., and Levelut, A. M., 1990, *Organometallics*, **9,** 2028.
[8] Baena, M. J., Espinet, P., Ros, M. B., and Serrano, J. L., 1996, *J. mater. Chem.*, **6,** 1291.
[9] Versace, C., Bartolino, R., Ghedini, M., Neve, F., Armentano, S., Petrov, M., and Kirov, N., 1990, *Liq. Cryst.*, **8,** 481.
[10] Alonso, P. J., and Martinez, J. I., 1996, *Liq. Cryst.*, **21,** 597.
[11] Levelut, A. M., Veber, M., Francescangeli, O., Melone, S., Ghedini, M., Neve, F., Nicoletta, F. P., and Bartolino, R., 1995, *Liq. Cryst.*, **19,** 241.
[12] Abied, H., Guillon, D., Skoulios, A., Dexpert, H., Giroud-Godquin, A. M., Maldivi, P., and Marchon, J., 1988, *J. de Phys.*, **49,** 345.
[13] Maldivi, P., Guillon, D., Giroud-Godquin, A. M., Marchon, J., Abied, H., Dexpert, H., and Skoulios, A., 1989, *J. chim. Phys.*, **86,** 1651.
[14] Barbera, J., Esteruelas, M. A., Levelut, A. M., Oro, L. A., Serrano, J. L., and Sola, E., 1992, *Inorg. Chem.*, **31,** 732.
[15] Weber, P., Guillon, D., and Skoulios, A., 1987, *J. phys. Chem.*, **91,** 2242.
[16] Vacus, J., Doppelt, P., Simon, J., and Memetzidis, G., 1992, *J. mater. Chem.*, **2,** 1065.
[17] Hoshino, N., Kodama, A., Shibuya, T., Matsunaga, Y., and Miyajima, S., 1991, *Inorg. Chem.*, **30,** 3091.
[18] Ghedini, M., Armentano, S., Bartolino, R., Korov, N., Petrov, M., and Nenova, S., 1988, *J. mol. Liq.*, **38,** 207.
[19] Levelut, A. M., Ghedini, M., Bartolino, R., Nicoletta, F. P., and Rustichelli, F., 1989, *J. de Phys.*, **50,** 113.
[20] Albertini, G., Guido, A., Mancini, G., Stizza, S., Ghedini, M., and Bartolino, R., 1990, *Europhys. Lett.*, **12,** 629.
[21] Barbera, J., Levelut, A. M., Marcos, M., Romero, P., and Serrano, J. L., 1991, *Liq. Cryst.*, **10,** 119.
[22] Martinez, J. I., Marcos, M., Serrano, J. L., Orera, V. M., and Alonso, P. J., 1995, *Liq. Cryst.*, **19,** 603.
[23] Szdlowska, J., 1996, *J. mater. Chem.*, **6,** 733.
[24] Zheng, H. X., Lai, C. K., and Swager, T. M., 1995, *Chem. Mater.*, **7,** 2067.
[25] Paschke, R., Diele, S., Letko, I., Wiegeleben, A., Pelzl, G., Griesar, K., Athanassopoulou, M. A., and Haase, W. H., 1995, *Liq. Cryst.*, **18,** 451.
[26] Abser, M. N., Bellwood, M., Holmes, M. C., and McCabe, R. W., 1993, *J. chem. Soc. chem. Commun.*, **13,** 1062.
[27] Abser, M. N., Bellwood, M., Buckley, C. M., Holmes, M. C., and McCabe, R. W., 1994, *J. mater. Chem.*, **4,** 1173.
[28] Abser, M. N., 1991, PhD thesis, Lancashire Polytechnic.
[29] Buckley, C. M., 1995, PhD thesis, University of Central Lancashire.
[30] Ohta, K., Morizumi, Y., Fujimoto, T., and Yamamoto, I., 1992, *Mol. Cryst. liq. Cryst.*, **214,** 161.
[31] Hanasaki, T., Ueda, M., and Nakamura, N., 1993, *Mol. Cryst. liq. Cryst. Sci. Tec. A*, **237,** 329.
[32] Chandrasekhar, S., 1994, *Mol. Cryst. liq. Cryst. Sci. Tec. A*, **243,** 1.
[33] Harris, C. M., Lenzer, S. L., and Martin, R. L., 1958, *Aust. J. Chem.*, **11,** 331.
[34] Goossens, W. J. A., 1985, *J. de Phys.*, **46,** 1411.
[35] El Sayed, L., and Iskander, M. F., 1971, *J. inorg. nucl. Chem.*, **33,** 435.
[36] Ubbelohde, A. R., 1978, *The Molten State of Matter* (Wiley), Chap. 7.
[37] Chandrasekhar, S., and Madhusudana, N. V., 1973, *Appl. Spec. Rev.*, **6,** 189.
[38] Fontana, M. P., 1991, *Physics of Liquid Crystalline Materials*, edited by I. Khoo and F. Simoni (Gordon and Breach), Chap. 5.
[39] Fontana, M. P., Anachkova, E., Monda, O., Rateo, M., Angeloni, A. S., and Laus, M., 1994, *Mol. Cryst. liq. Cryst.*, **243,** 31.